Contents lists available at ScienceDirect

Food and Bioproducts Processing

journal homepage: www.elsevier.com/locate/fbp

Application of moderate electric fields and CO_2-laser microperforations for the acceleration of the salting process of Atlantic salmon (*Salmo salar*)

Javier Olivares[a], *Helena Nuñez*[a,*], *Cristian Ramírez*[a,b], *Aldonza Jaques*[a], *Marlene Pinto*[a], *Lida Fuentes*[b], *Sergio Almonacid*[a,b], *Oscar Vega-Castro*[c], *Ricardo Simpson*[a,b]

[a] *Departamento de Ingeniería Química y Ambiental, Universidad Técnica Federico Santa María, Valparaíso, Chile*
[b] *Centro Regional de Estudios en Alimentos Saludables (CREAS), CONICYT-Regional GORE Valparaíso Proyecto R17A10001, Avenida Universidad 330, Placilla, Curauma, Valparaíso, Chile*
[c] *BIOALI Research Group, Department of Food, Faculty of Pharmaceutical Sciences and Food, Universidad de Antioquia, Medellín, Colombia*

ARTICLE INFO

Article history:
Received 9 June 2020
Received in revised form 21 August 2020
Accepted 26 October 2020
Available online 4 November 2020

Keywords:
Salting
Salmon (*Salmo salar*)
Moderate electric field
CO_2laser microperforations
Mathematical modeling
Salt diffusion

ABSTRACT

The main limitation of salting is its extended processing time, mainly caused by the slow diffusion of salt into the muscle tissue. The diffusion process can be accelerated by different technologies such as moderate electric fields (MEF) and CO_2-laser microperforations.

The main objective of this research was to evaluate the implementation of a combined MEF-CO_2-laser-microperforation treatment on the acceleration of the salting process in Atlantic salmon (*Salmo salar*) and its influence on the effective diffusion coefficient (D_{eff}).

Salmon fillets were cut in cylinders. Microperforations at 50 and 100% depth into salmon tissue were produced axially with a 100 W CO_2 laser. For MEF treatment an electric field strength of 1 V/cm was used. Salt concentrations along time were analyzed through Fick's second law and anomalous diffusion models, considering a finite cylindrical geometry.

As a result, treatment with micropores-MEF achieved a salt concentration of 3.5% after 4 h, while the control required 12 h to reach the same salt concentration. When both technologies were simultaneously applied, both D_{eff} and final equilibrium salt concentration were increased, thus resulting in a significant reduction in salting time. The mathematical analysis showed good fit through the anomalous, presenting a sub-diffusive ($\alpha < 1$) behavior for all treatments.

1. Introduction

The main limiting factor of the brine-salting procedure is prolonged processing time. The processing time is approximately 48 h and limited principally by two factors, namely, low salt diffusion in muscle tissues and low temperatures (Van Nguyen et al., 2010). The mechanism involved in salting fish indicates that salt migration by diffusion plays an essential role (Wang et al., 2000). Salt diffusion is significantly reduced at low temperatures (Gou et al., 2003), but due to a long processing time, salmon salting must be carried out at low temperatures of 2–4 °C (Birkeland and Bjerkeng, 2005).

The evaluation of MEF in food processing includes studies on fruits, fish and pork meat (Simpson et al., 2015, 2018; Hong et al., 2012; McDonnell et al., 2014; Núñez et al., 2020). During osmotic dehydration of an apple, the MEF accelerated mass transfer significantly and reduced the processing time (Simpson et al., 2015). In salmon, the brining process coupled to MEF showed no significant differences in the effective diffusion coefficient (D_{eff}) of salt within salmon tissue compared to that of standard procedures. However, MEF technology has demonstrated up to an 80% reduction in the salting processing time of salmon using a shallow electric field (~2 V/cm). This reduced process-

* *Corresponding author.*
E-mail address: helena.nunez@usm.cl (H. Nuñez).
https://doi.org/10.1016/j.fbp.2020.10.014

ing time increases the salt concentration of the final product and does not affect the final product quality (Simpson et al., 2018).

Another emerging, albeit less well-studied, technology to generate microperforations is the carbon dioxide (CO_2) laser beam. This technology can be applied at specific locations, within a diameter ranging from 50 to 300 μm, and on several surfaces and arrangements (Yelden Eugene and David, 2008; Altshuler et al., 2000). Furthermore, it is a non-contact technology that significantly diminishes the chance of physical and microbiological contamination of materials, as observed with traditional cutting or contact with devices or fluids (Bilanski and Ferraz, 1991; Ferraz et al., 2007). To date, few applications have been reported in the food industry. Some of these applications include the use of CO_2-laser in potato peeling (Bilanski and Ferraz, 1991) and tomato peeling (Silva-Vera et al., 2020), browning of doughs in baking processes (Blutinger et al., 2019), product identifications on the surface of avocados and grapefruits (Sood et al., 2009) and on eggshells (Chen et al., 2009a, 2009b), creating channels for faster water penetration in the form of accelerating tempering in wheat (Hou et al., 2009), and accelerating diffusion in the impregnation process in frozen blueberry skin as a pretreatment of osmotic dehydration (OD) (Fujimaru et al., 2012). In frozen blueberries, the application of CO_2-laser microperforations improves water removal with concomitant sugar infusion during skin pretreatment of blueberries that were mechanically cut (Fujimaru et al., 2012). This application has also demonstrated significant potential as a skin pretreatment for the freeze-drying of blueberries (Munzenmayer et al., 2020).

The mathematical model of the salt diffusion process during brining has presented some deviations from Fick's second law mainly due to the heterogeneous microstructure of salmon tissue. However, as reported by Simpson et al., (2018), the use of MEF to accelerate the brining process deviates even further from the diffusion process, being necessarily considered an anomalous model to describe the phenomena better, being fractional calculus a powerful tool to apply in this type of case. It is challenging to adequately represent the diffusion in microperforated salmon tissue salting by MEF using fractional calculus. To date, no application of CO_2-laser microperforation on salmon salting has been reported, nor is there information on the mathematical modeling of the diffusion process.

The main objective of this research was to evaluate the implementation of a MEF-CO_2-laser combined treatment on the acceleration of the salting process in Atlantic salmon (*Salmo salar*) and its influence on the effective diffusion coefficient (D_{eff}) as determined using Fick's second law and an anomalous diffusion model considering a finite cylinder geometry.

2. Materials and methods

2.1. Sample preparation

Atlantic salmon fillets (*Salmo salar*) were acquired from a local market and transported in an insulated box to the laboratory under refrigeration (2 °C). Three salmon fillets were used for each experiment. The fillets were cut to simulate finite cylinders of 0.04 ± 0.001 m in diameter and 0.007 ± 0.001 m in height, and the weights of the resulting samples of salmon were 8 ± 0.005 g. Each sample was weighed, tagged and immediately processed.

2.2. Brining and sampling

The samples were randomly collected and salted by immersion in 6% solution (w/w). The salting solution was prepared using food grade NaCl and tap water at a brine/salmon ratio (11/1 w/w) high enough to avoid any significant concentration change in the brine solution during the salting experiments (Simpson et al., 2018). For the salting process, the samples were immersed in a tank containing two concentric cylindrical stainless-steel electrodes of 3.7 and 19 cm in diameter with 7.65 cm between them. The tank had a nonconducting plastic bottom. To prevent the samples from floating during the experiments, a plastic grid was used to keep them submerged. The salting processes were conducted at 6 ± 2 °C for 24 h. The temperature and voltage were measured with copper wire thermocouples connected to an OM-320 data logger (Omega Engineering, Stamford, CT, USA) using a modem connection and port connection to a computer. For MEF treatment, an electric field strength (E) of 1 V/cm was used (Simpson et al., 2018). To calculate the yield during salmon salting, samples (n = 3) were analyzed after drainage for 2–3 min on a grid at different sampling times (0, 0.5, 1, 1.5, 2, 4, 8, 12, and 24 h). At each timepoint, three cylinders of salmon were randomly chosen, and their salt concentration and water content were separately determined.

Six salting treatments were carried out, as follows: a) standard sample salting as a control process, b) microperforated samples with CO_2-laser with 50% depth of salmon tissue (depth breakthrough of 3.5 mm) followed by standard salting, c) microperforated samples with CO_2-laser with 100 % depth of salmon tissue (depth breakthrough of 7 mm) followed by standard salting, d) salting coupled with the application of MEF, e) microperforated samples with CO_2-laser (50%) followed by salting coupled with the application of MEF, and f) microperforated samples with CO_2-laser (100%) followed by salting coupled with the application of MEF. The schematic representation of the experimental design is presented in Fig. 1.

2.3. Microperforations with CO_2 laser technology

Sample preparation for samples with microperforations were done with a 100 W CO_2 laser (Firestar t100, Synrad Inc. Mukilteo, Wash., USA) with a 1500-mm focus, FLA-125 lenses (Serial # 1859), and a computer interface with WinMark Pro laser market software (Synrad Inc.). The system was operated at a continuous wavelength of 10.6 μm and a frequency of 10 kHz. Samples were perforated at 50 and 100% depth into the salmon tissue. Both were an 8 × 8 microperforation matrix with a 5-mm gap between each perforation, made with a FLA-125 (Serial # 1859) lens. The pore size was of 233 ± 17.50 μm. In the case of 50% depth, the following parameters were set in the laser equipment: 10% power, 400 pulses and pulse time of 3 μs with a time between pulses of 4 μs; on the other hand, for 100% perforation, the following parameters were used: 12% power, 400 pulses and pulse time of 3 μs with a time between pulses of 6 μs.

2.4. Analysis of the sample composition

The moisture content $\left(X_t^W\right)$ was determined by drying the samples (n = 3) according to the method defined by the Association of Official Analytical Chemists (Association of official analytical chemist (AOAC, 1996). The salt concentration of each sample was measured in triplicate using a DiCromat II Salt Analyzer (PCL Control Instrument, Leicester, UK).

Changes in the salt and water contents (ΔM_t^W and ΔM_t^{NaCl}, respectively) were calculated using the following equations:

$$\Delta M_t^W = \frac{M_t^0 x_t^W - M_0^0 x_0^W}{M_0^0}, \tag{1}$$

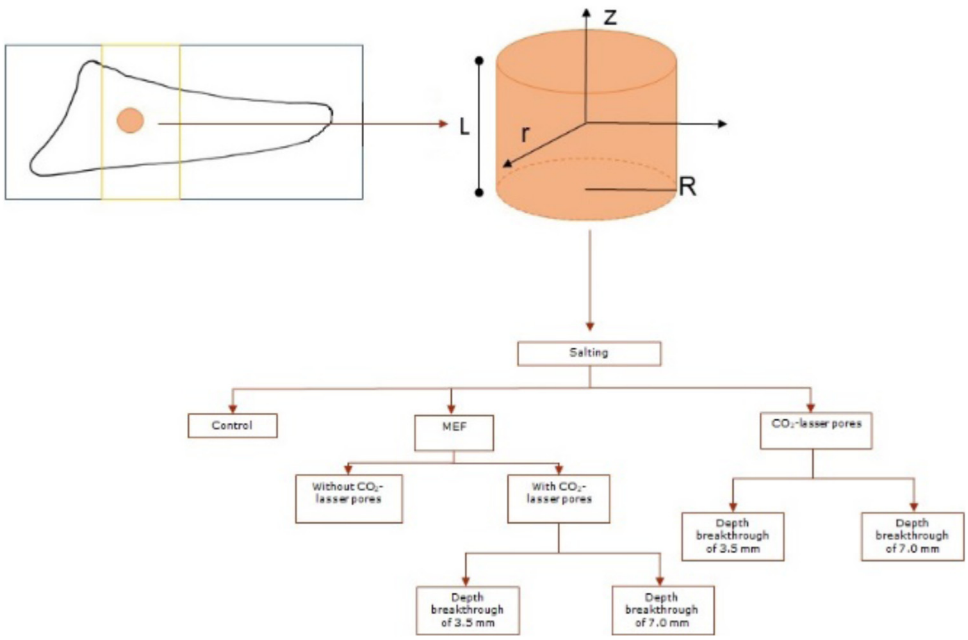

Fig. 1 – Schematic representation of the experimental design of salmon cylinder salting using brining solution.

$$\Delta M_t^{NaCl} = \frac{M_t^0 x_t^{NaCl} - M_0^0 x_0^{NaCl}}{M_0^0} \tag{2}$$

where M_0^0 and M_t^0 represent the sample weight at times 0 and t, respectively; and x_0^w, x_t^w, x_0^{NaCl}, and x_t^{NaCl} are the water (W) and salt (NaCl) mass fractions in a given sample at times 0 and t, respectively.

2.5. *Mathematical analysis of the salmon brining process*

2.5.1. *Fick's second law model*

Salmon tissue can be considered to have a heterogeneous structure (4; Sigurgisladottir et al., 2000), where the diffusion process in porous materials can be expressed in terms of the effective diffusivity (D_{eff}) (Simpson et al., 2018). This corresponds to an observed parameter, which represents salting by a diffusive process. The geometry for the salmon sample used here was a finite cylinder. The average concentration progress of the sample can be determined by combining the analytical solution of Fick's second law for the diffusion process in an infinite cylinder with that of an infinite slab. The mathematical description for diffusion in a finite cylinder is given by Eq. (3):

$$\frac{\partial C}{\partial t} = D_{eff} \frac{1}{r}\frac{\partial}{\partial r}\left(r\frac{\partial C}{\partial r}\right) + D_{eff}\left(\frac{\partial^2 C}{\partial z^2}\right) \tag{3}$$

where C is the average solute concentration in the salmon, r and z are the radial and axial directions (m), respectively, D_{eff} is the effective diffusion coefficient (m^2/s) in the tissue, and t is time (s). The solution of Eq. (3) depends on the initial conditions:

$$C(r, z, 0) = C_0 \tag{4}$$

and boundary conditions,

$$C(r = R, z, t) = C(r, z = \pm L/2, 0, t) = C_e,\ t > 0 \tag{5}$$

where C_0 is the initial concentration and C_e is the equilibrium salt concentration (considered to be the surface boundary condition). It is important to remark that Ce do not correspond to the concentration of brine solution, otherwise Ce is the salmon tissue concentration in equilibrium with the brine concentration. Ce used for fitting corresponded to that attained at 24 h.

The dimensionless average concentration for a finite cylinder is given by the integration of Eq. (3) (Crank, 1975).

$$C^* = \frac{8}{\pi}\left[\sum_{n=1}^{250}\frac{1}{2n-1}\exp\left(-D_{eff}\left(\frac{(2n-1)\pi}{L}\right)^2 t\right)\right] \left[\sum_{n=1}^{250}\frac{4}{\varepsilon_n^2}exp\left(\frac{-\varepsilon_n^2 D_{eff}}{R^2}t\right)\right] \tag{6}$$

where C* is the normalized average of the salt content present in salmon cylinders and is defined as $C^* = (\overline{C}(t) - C_e)/(C_0 - C_e)$; L is the half-thickness (m); ε_n is the nth root of the equation $J_0(\varepsilon_n) = 0$; R is the cylinder radius (m); and n is the number of terms used for summation (for this study case, the number of terms corresponded to 250).

2.5.2. *Anomalous diffusion model*

The use of fractional time derivatives has been confirmed by studies that indicate that porous materials can be well-characterized with respect to superdiffusive and subdiffusive behavior using only temporary fractional orders (Simpson et al., 2013). Thus, the solution for the anomalous diffusion is shown in Eq. (7).

$$\frac{\partial^\alpha C}{\partial t^\alpha} = D_{eff}^* \frac{1}{r}\frac{\partial}{\partial r}\left(r\frac{\partial C}{\partial r}\right) + D_{eff}^*\left(\frac{\partial^2 C}{\partial z^2}\right) \tag{7}$$

Temporal fractional calculus was considered to approach diffusion in which the value of α is associated with the anomalous order. The value of α depends on the food product and represents the fractional kinetics indicating if the diffusion process is subdiffusive, if $0 < \alpha < 1$, or is defined as superdiffusive, when $\alpha > 1$. In the case where $\alpha = 1$, the model is described by Fick's second law. D^*_{eff} is the fractional diffusion coefficient (m/s^α), where the same boundary conditions (Eqs. (4) and (5)) for Fickian diffusion are applied. Then, the solution for the anomalous diff ;usion model is shown in Eq. 8.

$$C^*_f = \frac{8}{\pi}\left[\sum_{n=1}^{\infty 250}\frac{1}{2n-1}E_{\alpha,1}\left(-D^*_{eff}\left(\frac{(2n-1)\pi}{L}\right)^2 t^\alpha\right)\right]\left[\sum_{n=1}^{250}\frac{4}{\varepsilon_n^2}E_\alpha\left(\frac{-\varepsilon_n^2 D^*_{eff}}{R^2}t^\alpha\right)\right] \quad (8)$$

where Eα corresponds to a Mittag-Leffler function (Ramírez et al., 2016), which corresponds to the following equation.

$$E_\alpha(z) = \sum_{k=0}^{\infty}\frac{z^k}{\Gamma(\alpha k+1)} \quad (9)$$

2.6. Determination of the effective diffusion coefficient (D_{eff} and D^*_{eff}) and statistical analysis

MATLAB R2019a software, version 9.6 (The MathWorks, Inc., Natick, MA, USA) was used to perform the nonlinear regression of the experimental data, minimizing the sum of the least squares and obtaining the D_{eff} values. The following objective function was used:

$$F_{objective}\left(D_{eff}, Ce\right) = \sum_{i=1}^{n}\left(C^*(t)_{calculated} - C^*(t)_{experiment}\right)^2 \quad (10)$$

For anomalous diffusion (Eq. (8)), the same formula (Eq. (10)) is used. However, in this case, two parameters (D^*_{eff} and α) are obtained from the fitted data.

$$F_{objective}\left(D^*_{eff}, \alpha, Ce\right) = \sum_{i=1}^{n}\left(C^*_f(t)_{calculated} - C^*_f(t)_{experiment}\right)^2 \quad (11)$$

The adjusted coefficients of determination (R^2) for both were calculated to account for the difference in the number of parameters, where n is the sample size and p is the number of parameters of the respective adjustment.

$$R^2 = 1 - (n-1)/(n-p)\cdot F_{objetive} \quad (12)$$

Comparison of $\left(R^2\right)$ allows for consideration of the overfit and thus comparison of the regression models using a different number of parameters: D_{eff} for a Fickian model (Eq. 6) and D^*_{eff},α for an anomalous model (Eq. 8).

3. Results and discussion

3.1. Salt and water mass change

Fig. 2A shows the salt weight changes (ΔM_t^{NaCl}) in salmon muscle during brining. There was a significant salt increase ($p < 0.05$) from initial values of 0.28 ± 0.01 up to values of 4.38 ± 0.02 in control and MEF-100% samples, respectively, by the end of the process (24 h). Treatment with MEF resulted in products with higher salt concentrations compared to the control sample; this can be explained by the effect of electroporation (Hong et al., 2012; Kusnadi & Sastry, 2012), the same kind of effect has also been reported in salmon by Simpson et al. (2018). When

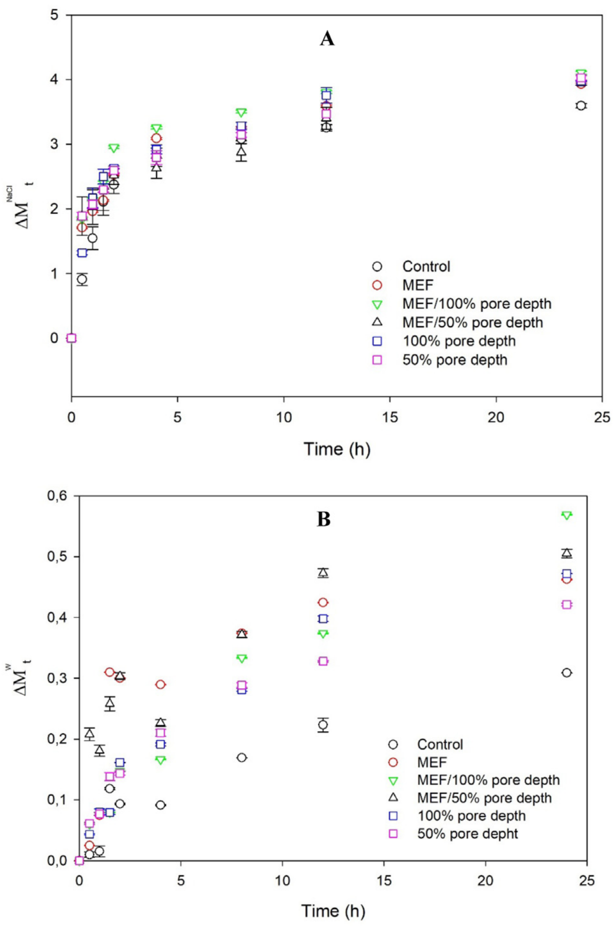

Fig. 2 – Weight changes during the salting time of salmon cylinders for (A) salt and (B) water.

microperforation only was used, there were significant differences between the experimental and control treatments ($p < 0.05$), which suggests that laser perforation was more effective in promoting salt gain; however, there was no statistical significance between the depths. A study by Fujimaru et al. (2012) investigated the utility of CO_2 laser perforation as a novel skin pretreatment for the sugar infusion of blueberries and demonstrated that laser perforation can be a viable skin pretreatment technique. However, the effect of laser perforation processes has not been studied in fish.

Significant interaction was observed between MEF and microperforation treatment, obtaining the highest salt weight change in MEF treatment with 100% depth, which suggests a combined effect of electroporation and laser perforation, especially when deeper penetration is used.

Fig. 2B shows the water weight changes (ΔM_t^w) in brined salmon samples. The samples brined at 6% (w/w) gained water throughout the brining process; similar results have been reported by Aursand et al. (2010), Gallart-Jornet et al. (2007a, 2007b) and Jiang et al. (2019).

The results show that the salting treatment, MEF or microperforation, significantly affected the water weight change in the samples. The effect of water weight change was greater with MEF than with microperforation application up to 12 h. One possible explanation is that the electroporation is reversible due to the low concentration of brine (6%); therefore, it allows the salt to enter, saturating the interior of the cell, and subsequently, water enters to reach an osmotic balance. Treatment with microperforations causes a greater increase in water weight than the control treatment. This can

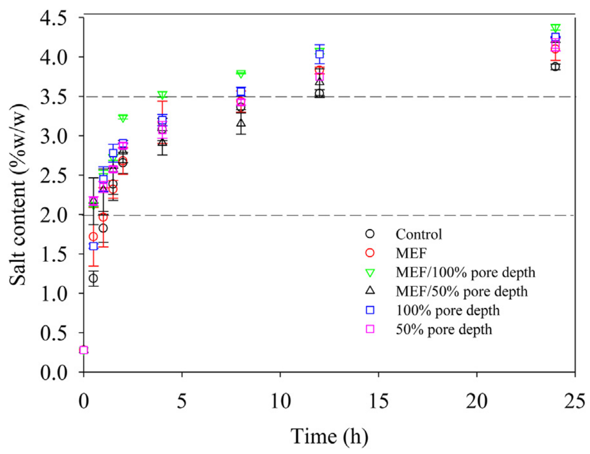

Fig. 3 – Salt content attained in samples of salmon over time salted with brining solution at 6% w/w.

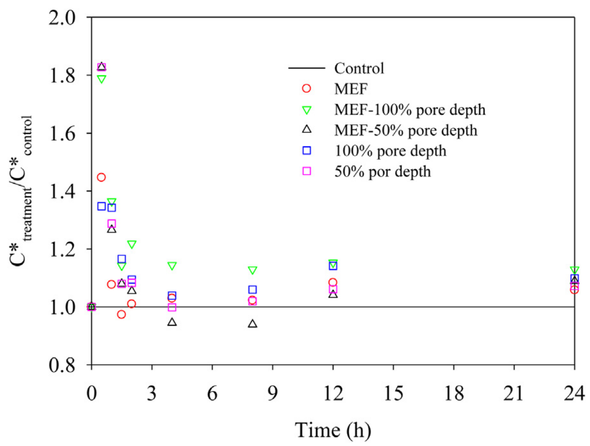

Fig. 4 – Comparative plot of the control versus all treatments.

be explained by the increased porosity caused by the laser, which favors the migration and retention of solution within the salmon samples. The electroporation effect is increased with microperforation treatment, obtaining the highest water retention capacity in the case of MEF-100%.

3.2. Effect of micropores and MEF on the salt content of salmon samples

The results obtained for the salt content of salmon cylinders during 24 h of salting are depicted in Fig. 3. At first glance, it is possible to observe differences between treatments, mainly where micropores with 100% of depth coupled with MEF were performed. These differences are visualized by plotting the control versus all treatments (Fig. 4). This plot demonstrates that the MEF-100% pore is the faster treatment. As shown in Figs. 3 and 4, if a threshold of 3.5% salt is used, the MEF-100% pore depth attained this value in only 4 h, while all other treatments attained this value in the range of 8 h (100% without MEF) to 10 h (MEF-50%, 50%) and even 12 h (control).

However, if we further analyze the curves, a second threshold at 2% salt is evident. All treatments with micropores and micropores coupled with MEF attained this value in approximately 30 min, while the control and MEF required at least 60 min to attain 2% salt. Therefore, during the first hours of processing, 50% and 100% pore depth behaved similarly in terms of salt diffusion to salmon tissue. However, as time elapsed, significant differences developed between both treatments. These differences can be attributed to the capacity of micropores with respect to the content of brining solution. The micropore diameter was approximately 233 μm x3.5 mm deep (50% pore depth) and 233 μm x7 mm deep (100% pore depth), which resulted in a volume capacity of 0.015 mL and 0.030 mL per micropore, respectively. If we considered an array of 8 × 8 pores, (64 micropores per sample), the maximum volume of solution in the sample is 0.96 mL and 1.92 mL, respectively. This implies that an amount of 0.0575 g for 50% pore depth and 0.115 g of salt for 100% pore depth can be introduced easily into each sample. This therefore explains the differences in Ce attained after 24 h in the salting process.

In general, the use of CO_2 laser-based micropores has been reported as a technique to accelerate mass transfer. For example, Almonacid et al. (2020) applied pores over blueberry surfaces to accelerate the mass transfer during the freeze-drying process and found that the primary drying time can be significantly reduced from 17 h to 13 h when nine micropores were introduced over blueberry skin. The quality of the dehydrated blueberry was significantly increased by reducing the burst effect. Other studies also showed the positive effect of micropores on the mass transfer process developed by Silva-Vera et al. (2020). The results showed a positive effect on NaOH transfer through tomato skin when it was micro drilled, which can be summarized in a reduced peeling time and a reduction in the NaOH concentration and waste-water strength.

MEF has also been studied as a method to accelerate mass transfer in osmotic dehydration and salting using brining solution. For example, Simpson et al. (2018) evaluated the effect of MEF in salting of salmon samples using brining solutions at different concentrations. Their results showed that the salt concentration increased when MEF was applied due to electroporation of the cell structure, reducing the time required to obtain a specific salt content (2% w/w). For example, obtaining 2% w/w of salt using a brining solution of 6% w/w without MEF took 2.5 h, while applying MEF only took 1.4 h. Additionally, MEF modified the equilibrium salt concentration attained by salmon samples and was significantly higher than the control. However, the D_{eff} did not significantly differ between the MEF and control groups. Therefore, the authors concluded that boundary conditions are important for the diffusion process rather than the salt migration inside the tissue.

3.3. Mathematical analysis based on Fick's second law and the anomalous diffusion model

The mathematical analysis based on Fick's second law and the anomalous diffusion model based on fractional calculus for the salt content in salmon samples over time using different combinations of micropore depth and MEF are summarized in Tables 1 and 2, respectively.

Fick's second law was used to model the data obtained from different experiments. In general, the adjusted experimental data delivered R^2-adjusted values in the range of 0.842 to 0.978, with RMSE varying between 0.177 and 0.441. The results showed that the best fit was obtained for control samples (R^2 = 0.974) and MEF (R^2 = 0.978) treatment. Other treatments with physical changes (samples with micropores) could produce even more deviation with respect to the Fickian diffusion process, especially in cases with 50% micropore depth, which presented lower R^2 values (Fig. 5A). The results for D_{eff} showed that MEF did not present significant differences with respect to the control process, with values of 3.43×10^{-10} m^2/s and 3.53×10^{-10} m^2/s, respectively. However, a non-significantly (p

Table 1 – Fick's second law model parameters obtained for different treatments of the salmon brining process.

	Fick's second law model										
Treatments	D_{eff} x 10^{10} m^2/s					*Ce* experimental (% w/w)				RMSE	R^2-adjusted
Control	3.53	±	0.467	a	a	3.87	±	0.04	a	0.192	0.974
MEF	3.43	±	0.652	a	b	4.10	±	0.14	b	0.177	0.978
MEF-100%	4.90	±	0.184	a	c,d	4.37	±	0.04	c,d	0.25	0.96
MEF-50%	4.03	±	0.729	a	b,d	4.22	±	0.04	b,d	0.441	0.842
100%	4.04	±	0.243	a	b,d	4.26	±	0.01	b,d	0.263	0.955
50%	4.23	±	0.728	a	b	4.15	±	0.08	b	0.344	0.907

*Different lowercase letters represent significant differences between treatments ($p < 0.05$).

Table 2 – Anomalous model parameters obtained for different treatments of the salmon brining process.

	Anomalous model													
Treatments	D_{eff} x 10^{-10} m^2/s^{α}				α				*Ce* experimental (% w/w)				RMSE	R^2-adjusted
Control	8.15	±	1.18	a	0.91	±	0.003	a	3.87	±	0.04	a	0.176	0.978
MEF	8.26	±	1.40	a	0.90	±	0.008	a	4.10	±	0.14	b	0.094	0.994
MEF-100%	49.92	±	5.84	b	0.74	±	0.009	c	4.37	±	0.04	c,d	0.104	0.993
MEF-50%	102.28	±	10.29	c	0.65	±	0.001	b	4.22	±	0.04	b,d	0.206	0.970
100%	30.25	±	8.27	b	0.78	±	0.024	e	4.26	±	0.01	b,d	0.168	0.982
50%	106.44	±	15.24	c	0.65	±	0.002	b	4.15	±	0.08	b	0.127	0.987

*Different lowercase letters represent significant differences between treatments ($p < 0.05$).

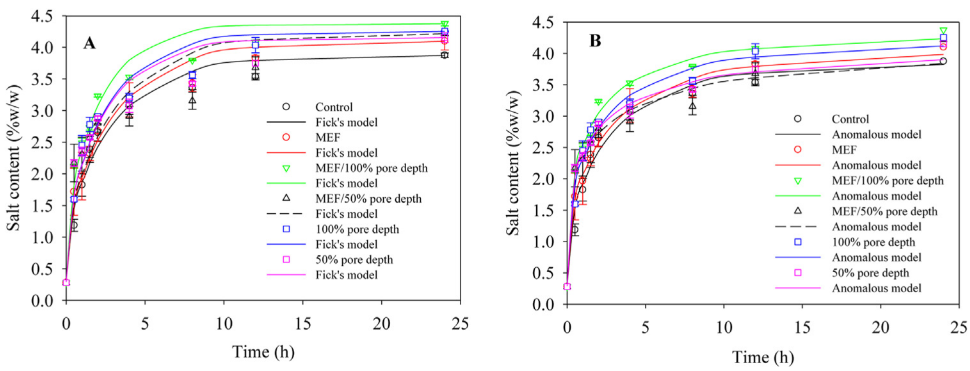

Fig. 5 – Salt content attained in salmon samples along the brining process modeled with: (A) Fick's second law and (B) anomalous diffusion model using fractional calculus.

> 0.05) increase can be observed when micropores (100% and 50% of depth) were generated, attaining maximum D_{eff} values of 4.90 × 10^{-10} m^2/s for MEF-100% pore depth. With respect to the equilibrium concentration (*Ce*) obtained experimentally, the results showed a significant increment ($p < 0.05$) in the case of MEF and MEF with micropores, respect to control. In terms of D_{eff} of NaCl in fish meat, the values obtained for us are according to those reported by Van Nguyen et al., (2010) for cod loins (range from 4.0 × 10^{-10} to 5.45 × 10^{-10} m^2/s) and Gallart-Jornet et al. (2007a, 2007b) for salmon fillets (range from 5.2 × 10^{-10} to 9.9 × 10^{-10} m^2/s).

Certainly, the poor fit of the data to Fick's second law model suggest that the diffusion phenomenon has anomalous behavior, given by its structure but also due to the presence of pores. The analysis based on the anomalous model using fractional calculus is summarized in Table 2 and presented in Fig. 5B. The results showed a notable improvement in the fitted data, with R^2 values over 0.97 and RMSE in the range of 0.094 to 0.206. The fractional component of time (α) showed a sub-diffusive behavior for all treatments. For treatments control and MEF the values of α were around 0.90, however, for MEF-micropores and micropores, the α values were ranged between 0.65 and 0.78, and the lowest values (α = 0.65) were obtained by MEF-50% micropore depth and 50% micropore depth, which suggests that the presence of pores caused an alteration of the diffusant movement into the salmon tissue. This could be caused by a stagnation phenomenon of brining solution in the pore. In the case of MEF-100% micropore depth and 100% micropore depth, the α values were 0.74 and 0.78, respectively, which suggests a similar phenomenon of sub-diffusion. This can be the product of the conic shape at the end of a pore entering the tissue, thus favoring this stagnation phenomenon. In the case of MEF, reversible electroporation can explain the value of α = 0.90.

Traditionally, the mean squared displacement is taken as proportional to time, $\langle x^2 \rangle \sim t$, in a diffusion process, as described by Fick's law of diffusion. However, in complex systems, as in biological materials, this situation does not hold, and the dependence of the mean square displacement is proportional to a power law in time, $\langle x^2 \rangle \sim t^{\alpha}$. Here, $\alpha < 1$ corresponds to subdiffusion, $\alpha > 1$ corresponds to superdiffusion, and $\alpha = 1$ is Fickian diffusion. The subdiffusion/superdiffusion nature does not indicate that the process is faster or slower. This nature is instead associated with the stochastic pro-

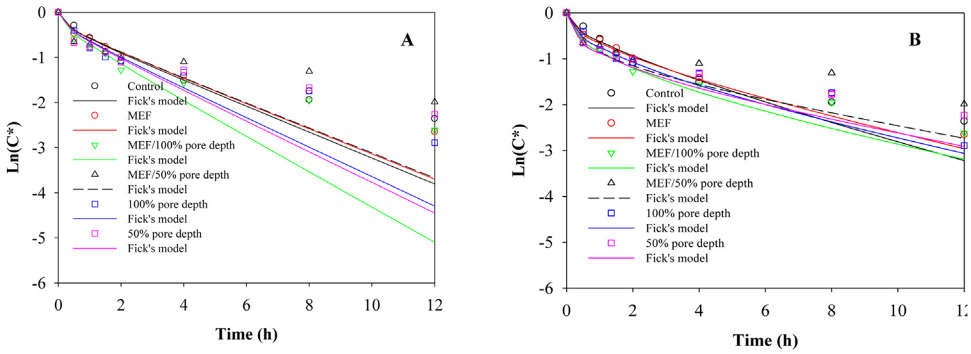

Fig. 6 – Logarithmic salt content attained in samples of salmon along the brining process as modeled with: (A) Fick's second law and (B) anomalous diffusion model using fractional calculus.

cesses on a microscale such that subdiffusion suggests a more dispersive pattern of diffusion and super diffusion a more channeled pattern of diffusion (Klafter and Sokolov, 2005).

The above analysis can be enriched by the analysis of D_{eff} and Ce attained by the modeling. The values of D_{eff} in the case of the control (8.15×10^{-10} $m^2/s^{0.91}$) and MEF (8.26×10^{-10} $m^2/s^{0.90}$) were similar, which is attributed to the time exponent close to 1. For MEF-100% micropore depth and 100% micropore depth, the D_{eff} values obtained were significantly different. D_{eff} was higher with both technologies simultaneously and even showed a synergistic effect with a D_{eff} value of 49.92×10^{-10} $m^2/s^{0.74}$ compared to micropores only where the D_{eff} was 30.25×10^{-10} $m^2/s^{0.78}$. However, an interesting result was obtained for MEF-50% micropore depth and 50% micropore depth, where the D_{eff} values were larger compared with the rest of the treatments, with values between 102.28×10^{-10} $m^2/s^{0.65}$ and 106.44×10^{-10} $m^2/s^{0.65}$ and reaching a Ce over 4.15%. The higher values of D_{eff} can be attributed to the fact that micropores of 50% depth are highly efficient during the first moments of salting due to a saturation of the pore wall with salt. However, as the process elapses, the solution of the medium cannot penetrate to the pore. For this reason, 50% micropore depth treatment up to 12 h presented low salt concentration, compared with the other treatments. At the end of 24 h, an increment in salt content is produced by structural damage due to the exposition time of salmon to the brining solution.

With respect to the fit of the models, it is possible to observe a significant difference between Fick's second law and the anomalous model when comparing the fit at the tails (end portions of the curves) of the mass transfer process (Figs. 5A and 5B). This difference is especially evident in a logarithmic scale (Figs. 6A and 6B). A Fickian diffusion approach is unable to satisfactorily represent the process, as the concentration tends towards the equilibrium salt concentration, independent of the number of terms used in sum, which has been reported as a limitation of Fickian diffusion (Simpson et al., 2013). Instead, an anomalous model approach based on fractional calculus successfully represents the findings, since it can be adjusted to accommodate the whole process, including the "heavy-tailed" kinetics (Simpson et al., 2013). These findings mean that cases in which the kinetic evolution annot be represented by the exponential kinetics associated to a traditional Fickian model. The fractional calculus approach has been successfully used in modeling the salting process in salmon (Nuñez et al., 2020). For anomalous diffusion it is required the use of an additional variable, fractional order α, together with fractional diffusion to describe the process.

4. Conclusions

Both MEF and CO_2 laser microperforations are novel technologies that can be applied separately or together to accelerate mass transfer in food matrices and to increase the yields of the diffusant entrance. In the case of MEF, there were no differences in the D_{eff} values with respect to the control. However, the equilibrium concentration, Ce, was significantly increased. With the application of CO_2 laser microperforations, both D_{eff} and the equilibrium concentration, Ce, were increased in salmon samples after 24 h. When both technologies were simultaneously applied, D_{eff} increased but not synergistically, which can be explained by the microstructural limitations related to cell structure and might determine the maximum D_{eff} value. Ce attained higher values due to the presence of micropores because brining solution was retained even when the samples were withdrawn from brining solution.

The mathematical analysis showed a good fit with the anomalous model, for both MEF or microperforations, even when both technologies were applied simultaneously. In all cases, there was a sub-diffusive character given that all the values of α were lower than 1.

Declaration of interests

The authors declare that they have no known competing financial interests or personal relationships that could have appeared to influence the work reported in this paper.

Acknowledgements

Authors Ricardo Simpson and Cristian Ramírez are grateful for the financial support provided by ANIDthough Fondecyt project numbers 1181270 and1191280, respectively.

References

Altshuler, G., Mass, B., Erofeev, A.V., Andrei, U.S. Patent 6015404, 18 January 2000 2000. Laser Dermatology with Feedback Control.

Association of Official Analytical Chemist (AOAC), 1996. Official Methods of Analysis, 16th ed, Washington, DC.

Aursand, I.G., Erikson, U., Veliyulin, E., 2010. Water properties and salt uptake in Atlantic salmon fillets as affected by ante-mortem stress, rigor mortis, and brine salting: a low-field 1H NMR and 1H/ 23Na MRI study. Food Chem. 120, 482–489.

Bilanski, W.K., Ferraz, A.C.O., 1991. Processing agricultural materials with a CO2 laser: a liner model. In: Proceedings of the International Winter Meeting, Chicago, IL, USA, 17–20 December, ASAE: Washington, DC, USA.

Birkeland, S., Bjerkeng, Bjørn, 2005. The quality of cold-smoked Atlantic salmon (Salmo salar) as affected by salting method, time and temperature. Int. J. Food Sci. Technol. 40, 963–976.
Blutinger, Jonathan David, Meijers, Yorán, Chen, Peter Yichen, Zheng, Changxia, Eitan, Grinspun, Lipson, Hod, 2019. Characterization of CO2 laser browning of dough. Innov. Food Sci. Emerg. Technol. 52, 145–157.
Chen, M.I., Hsiao, W.T., Huang, W.L., Hu, C.W., Chen, Y.P., 2009a. Laser coding on the eggshell using pulsed-laser marking system. J. Mater. Process. Technol. 209, 737–744.
Chen, M.F., Wang, Y.H., Hsiao, W.T., 2009b. Finite element analysis and verification of laser marking on eggshell. J. Mater. Process. Technol. 209, 470–476.
Crank, J., 1975. The Mathematics of Diffusion, second ed. Clarendon Press, Oxford, pp. 47–53.
Ferraz, A.C.O., Mittal, G.S., Bilanski, W.K., Abdullah, H.A., 2007. Mathematical modeling of laser based potato cutting and peeling. BioSystems 90, 602–613.
Fujimaru, T., Ling, Q., Morrissey, M.T., 2012. Effects of carbon dioxide (CO2) laser perforation as skin pretreatment to improve sugar infusion process of frozen blueberries. J. Food Sci. 77, E45–E51.
Gallart-Jornet, L., Barat, J.M., Rustad, T., Erikson, U., Escriche, I., Fito, P., 2007a. Influence of brine concentration on Atlantic salmon fillet salting. J. Food Eng. 80, 267–275.
Gallart-Jornet, L., Barat, J.M., Rustad, T., Erikson, U., Escriche, I., Fito, P., 2007b. A comparative study of brine salting of Atlantic cod (*Gadus morhua*) and Atlantic salmon (*Salmo salar*). J. Food Eng. 79, 261–270.
Gou, P., Comaposada, J., Arnau, J., 2003. NaCl content and temperature effects on moisture diffusivity in the Gluteus medius muscle of pork ham. Meat Sci. 63, 29–34.
Hong, G., Chun, J., Choi, M., 2012. Applications of low-voltage Ohmic process combined with temperature control system to enhance salting process of pork. Korean J. Food Sci. 32, 293–300.
Hou, G., Ling, Q., Zou, Y., Lee, B., 2009. Innovating a laser wheat-perforating technology to reduce kernel hardness for milling. In: Presented at AACC Intl. Annual Meeting, 2009 September 13–16; Baltimore, Maine.
Jiang, Q., Nakazawa, N., Hu, Y., Osako, K., Okazak, E., 2019. Changes in quality properties and tissue histology of lightly salted tuna meat subjected to multiple freeze-thaw cycles. Food Chem. 293, 178–186.
Klafter, Joseph, Sokolov, Igor M., 2005. Anomalous diffusion spreads its wings. Phys. World 18 (8), 29.
Kusnadi, C., Sastry, S.K., 2012. Effect of moderate electric fields on salt diffusion into vegetable tissue. J. Food Eng. 110, 329–336.
McDonnell, C.K., Allen, P., Chardonnereau, F.S., Arimi, J.M., Lyng, J.G., 2014. The use of pulsed electric fields for accelerating the salting of pork. LWT-Food Sci. Technol. 59, 1054–1060.
Munzenmayer, P., Ulloa, J., Pinto, M., Ramirez, C., Valencia, P., Simpson, R., Almonacid, S., 2020. Freeze-drying of blueberries: effects of carbon dioxide (CO2) laser perforation as skin pretreatment to improve mass transfer, primary drying time, and quality. Foods 9, 211.
Núñez, H., Cavada, G., Ramírez, C., Moreno, J., Jaques, A., Pinto, M., Vega, O., Simpson, R., 2020. Effect of a moderate electric field on the salting of atlantic salmon (salmo salar): an experimental study and phenomenological understanding. Food Res. Int. 137, 109475.
Sigurgisladottir, S., Sigurdardottir, M.S., Torrasen, O., Vallet, J.L., Hafsteinsson, H., 2000. Effects of different salting and smoking processes on the microstructure, the texture, and yield of Atlantic salmon (*Salmo salar*) fillets. Food Res. Int. 33, 847–855.
Silva-Vera, W., Avendaño-Muñoz, N., Nuñez, H., Ramírez, C., Almonacid, S., Simpson, R., 2020. CO2 laser drilling coupled with moderate electric fields for enhancement of the mass transfer phenomenon in a tomato (Lycopersicon esculentum) peeling process. J. Food Eng. 276, 109870.
Simpson, R., Jaques, A., Nuñez, H., Ramirez, C., Almonacid, A., 2013. Fractional calculus as a mathematical tool to improve the modeling of mass transfer phenomena in food processing. Food Eng. Rev. 5 (1), 45–55.
Simpson, R., Ramírez, C., Birchmeier, V., Almonacid, S., Moreno, J., Nuñez, H., Jaques, A., 2015. Diffusion mechanisms during the osmotic dehydration of granny smith apples subjected to a moderate electric field. J. Food Eng. 166, 204–211.
Simpson, R., Nuñez, H., Jaques, A., et al., 2018. Application of a moderate electric field for the potential acceleration of the salting process of Atlantic salmon (Salmo salar). J. Food Process Eng., e12846.
Sood, P., Ference, C., Narciso, J., Etxeberria, E., 2009. Laser etching: a novel technology to label Florida grapefruits. Horttechnolgy 19, 504–510.
Van Nguyen, M., Arason, S., Thorarinsdottir, K.A., Thorkelsson, G., Gudmundsdóttir, A., 2010. Influence of salt concentration on the salting kinetics of cod loin (Gadus morhua) during brine salting. J. Food Eng. 100, 225–231.
Wang, D., Tang, J., Correia, L.R., 2000. Salt diffusivities and salt diffusion in farmed Atlantic salmon muscle as influenced by rigor mortis. J. Food Eng. 43, 115–123.
Yelden Eugene, F., David, C., U.S. Patent 124433A1, 29 May 2008. Food Processing Using Laser Radiation.